

# Distributionally Robust Trajectory Optimization Under Uncertain Dynamics via Relative Entropy Trust-Regions

Hany Abdulsamad<sup>\*1</sup>, Tim Dorau<sup>\*1</sup>, Boris Belousov<sup>1</sup>, Jia-Jie Zhu<sup>2</sup>, *Member, IEEE*,  
and Jan Peters<sup>1</sup>, *Fellow, IEEE*

**Abstract**—Trajectory optimization and model predictive control are essential techniques underpinning advanced robotic applications, ranging from autonomous driving to full-body humanoid control. State-of-the-art algorithms have focused on data-driven approaches that infer the system dynamics online and incorporate posterior uncertainty during planning and control. Despite their success, such approaches are still susceptible to catastrophic errors that may arise due to statistical learning biases, unmodeled disturbances or even directed adversarial attacks. In this paper, we tackle the problem of dynamics mismatch and propose a distributionally robust optimal control formulation that alternates between two relative entropy trust-region optimization problems. Our method finds the worst-case maximum entropy Gaussian posterior over the dynamics parameters and the corresponding robust policy. We show that our approach admits a closed-form backward-pass for a certain class of systems and demonstrate the resulting robustness on linear and nonlinear numerical examples.

**Index Terms**—Optimal Control, Distributional Robustness, Trust-Region Optimization, Minimax Optimization, Time-Variant Systems, Dynamic Programming.

## I. INTRODUCTION

Trajectory optimization [1] is a well-established tool for solving control problems that rely on a model of the system dynamics to optimize a control signal that induces a desired system behavior. However, as systems of interest are getting more complex, involving nonlinear effects and high-dimensional state-action spaces, accurate analytical modeling has become hard if not impossible in some cases. Consequently, data-driven control approaches that employ black- and gray-box statistical models are becoming popular rapidly. However, trajectory optimization may exploit model imperfections that can arise as a result of statistical learning biases, resulting in brittle controllers that may fail at deployment time due to modeling discrepancies. The recent trend of over-reliance on learning from simulated data carries with it similar pitfalls w.r.t. optimization bias.

Advanced trajectory optimization and model predictive control (MPC) techniques successfully use learned probabilistic models to incorporate the uncertainty of data-driven learning [2], [3]. However, those approaches are not robust against

adversarial disturbances and general model mismatch. An alternative to such probabilistic modeling is the robust control paradigm. Unfortunately, robust methods tend to produce sub-optimal controllers on average because the disturbance model gives too much power to the adversary, forcing the controller to be too conservative. A new class of methods at the intersection of robust and stochastic optimal control is gaining momentum, based on distributionally robust optimization (DRO) [4]–[10], as it promises to combine the strengths of both approaches. In the DRO framework, one seeks to find a controller that performs optimally under a worst-case stochastic model chosen from a so-called ambiguity set. Here, the adversary’s strength is more limited compared to the classical robust control.

To make distributionally robust optimization practical, one needs to be able to infer the optimal adversary, i.e., find the worst-case stochastic system, in closed form or numerically. So far, closed-form solutions have been obtained only for special choices of the ambiguity set [11]. For example, when the ambiguity set is given as a relative entropy ball around a nominal distribution [12], [13]. In this paper, we build upon this insight to develop an algorithm for distributionally robust trajectory optimization.

We consider the problem of controlling a discrete-time stochastic dynamical system with transition density  $f(\mathbf{x}'|\mathbf{x}, \mathbf{u}, \boldsymbol{\theta})$  for which system uncertainty is encoded in the parameter distribution  $p(\boldsymbol{\theta})$  and the ambiguity set is given by the KL ball  $\mathcal{B}_\delta(\hat{p}) = \{p | \text{KL}(p || \hat{p}) \leq \delta\}$  centered around the nominal parameter distribution  $\hat{p}(\boldsymbol{\theta})$ , that we assume is available after a data-driven model learning phase. We seek a time-varying stochastic policy  $\pi_t(\mathbf{u}|\mathbf{x})$  that minimizes the worst-case expected cost  $\max_{p \in \mathcal{B}_\delta(\hat{p})} J(\pi, p)$ . In this setting, we develop an iterative trust region algorithm that alternates between optimizing the worst-case distribution  $p$  and the corresponding distributionally robust policy  $\pi$ . We derive optimality conditions for  $p$  and  $\pi$  and an efficient forward-backward procedure in the style of differential dynamic programming is provided for each optimization step.

The resulting method is applicable to nonlinear systems thanks to iterative local linearization. Empirical validation on uncertain linear and nonlinear dynamical systems demonstrates the robustness of the optimized policies against adversarial disturbances. Furthermore, we present an outlook to applying similar DRO principles to stochastic switching systems with the motivation of managing the size of exponentially growing mixtures by deriving an optimistic and a pessimistic state-filtering approach.

{\*} Equal Contribution. H. Abdulsamad, T. Dorau, B. Belousov, and J. Peters are with the Intelligent Autonomous Systems Lab, Technische Universität Darmstadt, Darmstadt, Germany. J.-J. Zhu is with the Data-driven Optimization and Control Group, Weierstrass Institute for Applied Analysis and Stochastics, Berlin, Germany. (e-mail: hany@robot-learning.de).

Our approach brings together several strands of research. First, we rely on distributionally robust optimization to find the worst-case parameter distribution. Second, our problem formulation is based on an iterative scheme of relative entropy policy search, a trust region algorithm for policy optimization [14]. Third, we employ iterative linearization and approximate integration to enable applications to nonlinear uncertain dynamical systems. Below, we highlight related work from these areas and point out key differences.

## II. RELATED WORK

Distributionally robust optimization finds numerous applications in control. Methods differ in ambiguity set representations, uncertainty, system modeling assumptions and optimization algorithms. In [6], the problem of controlling a linear system under distributionally robust chance-constraints was tackled using a moment-based ambiguity set. The moment-based representation was also employed in [10] to derive high-probability guarantees for stability of a linear system with multiplicative noise. For Wasserstein-based ambiguity sets, a general formulation was given in [8], which however requires solving a semi-infinite problem numerically, while we obtain a closed-form solution instead. Furthermore, a Wasserstein-based ambiguity set on the noise distribution was used to solve a data-enabled control problem in [7]. For the linear-quadratic case, a relaxed version was solved in [15] via a modified Riccati equation. The model, however, only included ambiguity over the additive noise while the rest of the dynamics were assumed known and time-invariant. In this paper, in contrast, we employ a time-varying linearized probabilistic dynamics model and allow ambiguity in the distribution over all parameters of the model.

Ambiguity sets based on relative entropy were also employed in a number of prior works. Distributionally robust optimization of stochastic nonlinear partially observable systems with relative entropy constraints was studied in a general abstract setting in [13]. In contrast to our work, the ambiguity set was formulated on the space of path measures, whereas we consider ambiguity sets on the space of parameter distributions of the underlying dynamical system. In [16], a formulation for nonlinear systems was presented where the uncertainty in the additive disturbance was ambiguous. Through Lagrangian duality, a connection to risk-sensitive control was furthermore established. This connection was recently used to derive a model predictive control algorithm [17] that builds upon iterative linear exponential quadratic Gaussian method (iLEQG) [18] and employs cross-entropy methods (CEM) to optimize the risk-sensitivity parameter, thereby obtaining the worst-case distribution. In contrast, our algorithm uses a principled approach based on our trust-region optimization to solve the resulting DRO problem. Finally, our DRO formulation captures the uncertainty in the whole trajectory, rather than considering only the noise distribution. This feature gives the adversary additional freedom in allocating the disturbance budget along the trajectory to critical time-steps.

Our approach builds upon relative entropy policy search (REPS) [14] by extending it with an adversarial optimization

with respect to the ambiguous distribution over the dynamics parameters. A risk-sensitive formulation based on REPS involving the entropic risk measure in a model-free setting was considered in [19]. In this paper, we instead work in a model-based setting [20] and optimize a controller under the worst-case distribution instead of the nominal one. Furthermore, we introduce an additional approximate state propagation step to accommodate for uncertainty in the dynamics parameters.

Stochastic optimal control with linearized dynamics [1], [21] is a powerful technique for controlling nonlinear systems. By using first-order approximations of the dynamics along a given trajectory, a locally optimal controller can be found via dynamic programming techniques. Using the updated controller to generate a new reference trajectory, the process is then iterated until convergence.

As the linearized dynamics is only a good approximation around the linearization point, it is important to limit the optimism in the controller updates. One successful approach has been to enforce a relative entropy bound between the trajectory distributions of successive iterations. This technique is used for trajectory optimization in the context of guided policy search (GPS) [20] and is dubbed maximum-entropy iterative linear quadratic Gaussian. Our approach relies on a similar formulation to optimize a time-variant policy, while considering uncertain dynamics.

In contrast to the aforementioned works, a distributionally robust approach not only considers the stochasticity captured by the probabilistic model, but also accounts for what is typically called *ambiguity*, meaning uncertainty about the probabilistic model itself.

## III. DISTRIBUTIONAL ROBUSTNESS

Robustness analysis studies the sensitivity of an optimization objective

$$\min_{\mathbf{x} \in \mathcal{X}} \max_{\boldsymbol{\theta} \in \Theta} J(\mathbf{x}, \boldsymbol{\theta})$$

with a decision variable  $\mathbf{x} \in \mathcal{X}$  w.r.t. to a parameter set  $\boldsymbol{\theta} \in \Theta$ . The solution  $\mathbf{x}^*$  is a conservative point that minimizes the worst-case objective w.r.t.  $\boldsymbol{\theta}$  and delivers an upper-bound on the objective  $J$  [11]. Furthermore, robust optimization assumes all parameters  $\boldsymbol{\theta} \in \Theta$  are equally probable.

In contrast, stochastic optimization assumes the parameters  $\boldsymbol{\theta}$  are random variables drawn from a known distribution  $p(\boldsymbol{\theta})$ . Thus, the objective  $J$  can be minimized under a distributional risk measure or an expectation operator for example

$$\min_{\mathbf{x} \in \mathcal{X}} \mathbb{E}_{p(\boldsymbol{\theta})} [J(\mathbf{x}, \boldsymbol{\theta})].$$

Distributionally robust optimization is a paradigm that combines the concepts of worst-case solutions and distributional uncertainty in one general framework. As in stochastic optimization the parameters  $\boldsymbol{\theta}$  are assumed to be random variables, however, the knowledge about the distribution  $p(\boldsymbol{\theta})$  is uncertain. An example of a distributionally robust optimization can be written as

$$\min_{\mathbf{x} \in \mathcal{X}} \max_{p \in \mathcal{P}} \mathbb{E}_{p(\boldsymbol{\theta})} [J(\mathbf{x}, \boldsymbol{\theta})],$$

where  $\mathcal{P}$  is a set over distributions, commonly referred to as the *ambiguity set*, and contains the worst-case distribution  $p^*(\theta)$  that upper-bounds the expected loss. The generality of this formulation becomes evident when we consider two different scenarios. In one scenario, the set  $\mathcal{P}$  may contain a single distribution, which recovers the stochastic optimization problem. In another,  $\mathcal{P}$  may contain all possible distributions with a support on  $\theta$ , thus delivering the classical robust optimization formulation.

The motivation behind distributional robustness considerations pertains to data-driven stochastic learning applications, where the distribution  $p(\theta)$  is hard to estimate due to limited data. Defining an ambiguity set and optimizing for the worst case is a robust approach to combat statistical learning biases and avoid catastrophic results.

Finally, the choice of the ambiguity set remains an important decision, as it directly influences the overall solution and its usefulness. Sets that are very broadly defined can lead to over-powered biases that cripple the optimization, while a restrictive set definition can undermine the robustness objective. Related literature includes a wide spectrum of possible definitions [11]. We focus on ambiguity sets defined using discrepancy measures w.r.t. a nominal distribution  $\hat{p}(\theta)$

$$\mathcal{P} := \mathcal{B}_\delta(\hat{p}) = \{p \mid D(p, \hat{p}) \leq \delta\},$$

where  $D$  is a measure of the distance or divergence between an arbitrary distribution  $p$  and the reference  $\hat{p}$ . The parameter  $\delta$  is the radius around  $\hat{p}(\theta)$ , which effectively bounds the worst-case scenario, or the severity of the worst possible case. More specifically, in this paper, we rely on the Kullback-Leibler divergence as a measure, due to its tractable computational properties and its compatibility with trust-region stochastic optimization.

#### IV. PROBLEM STATEMENT

In the scope of this paper, we concentrate on finite-horizon Markov decision processes (MDP) with a state space  $\mathcal{X} \subseteq \mathbb{R}^d$ , an action space  $\mathcal{U} \subseteq \mathbb{R}^m$ , and a time horizon  $T$ . We assume a probabilistic state transition density  $p(\mathbf{x}', \theta | \mathbf{x}, \mathbf{u}) = f(\mathbf{x}' | \mathbf{x}, \mathbf{u}, \theta)p(\theta)$ , where  $p(\theta)$  is a distribution over the dynamics parameters. The policy  $\pi_t(\mathbf{u} | \mathbf{x})$ , a time-variant conditional density, induces the state distribution  $\mu_t(\mathbf{x})$  according to transition dynamics.

In this setting, the stochastic optimal control objective can be written as

$$J(\pi_t, p) = \sum_{t=1}^{T-1} \int \int c_t(\mathbf{x}, \mathbf{u}) \mu_t(\mathbf{x}) \pi_t(\mathbf{u} | \mathbf{x}) d\mathbf{x} d\mathbf{u} \quad (1) \\ + \int c_T(\mathbf{x}) \mu_T(\mathbf{x}) d\mathbf{x},$$

where  $c(\mathbf{x}, \mathbf{u})$  is the cost function. This objective is constrained by the following integral equation describing the evolution of  $\mu_t(\mathbf{x})$  over time

$$\mu_{t+1}(\mathbf{x}') = \iiint \mu_t(\mathbf{x}) \pi_t(\mathbf{u} | \mathbf{x}) f(\mathbf{x}' | \mathbf{x}, \mathbf{u}, \theta) p(\theta) d\mathbf{u} d\mathbf{x} d\theta.$$

#### Algorithm 1: Dist. Robust Trajectory Optimization

**input** :  $\hat{\mu}_1, c_t, f, \hat{p}, \delta, \varepsilon, K$   
**initialize** :  $\pi_t^1$   
**for**  $k \leftarrow 1$  **to**  $K$  **do**  
     $p^{k+1} \leftarrow \text{worstCaseParamDist}(\hat{p}, \pi_t^k, \hat{\mu}_1, c_t, f, \delta)$   
     $\pi_t^{k+1} \leftarrow \text{robustPolicyUpdate}(\pi_t^k, p^{k+1}, \hat{\mu}_1, c_t, f, \varepsilon)$   
 $p^* \leftarrow p^{K+1}, \quad \pi_t^* \leftarrow \pi_t^{K+1}$   
**output** :  $\pi_t^*, p^*$

The distributionally robust trajectory optimization can then be written as a minimax problem over the distributions  $\pi_t(\mathbf{u} | \mathbf{x})$  and  $p(\theta)$

$$\underset{\pi_t}{\text{minimize}} \quad J(\pi_t, p^*), \quad (2a)$$

$$\text{subject to} \quad \int \pi_t(\mathbf{u} | \mathbf{x}) d\mathbf{u} = 1, \quad \forall \mathbf{x}, \forall t < T, \quad (2b)$$

where  $p^*(\theta)$  is the worst-case distribution given by

$$p^* := \arg \max_p J(\pi_t, p), \quad (3a)$$

$$\text{subject to} \quad \text{KL}(p(\theta) \parallel \hat{p}(\theta)) \leq \delta, \quad (3b)$$

$$\int p(\theta) d\theta = 1, \quad (3c)$$

where  $\hat{p}(\theta)$  is the nominal parameter distribution and  $\delta$  controls the size of the corresponding KL-based distributional ambiguity set.

The former robust optimization problem is typically hard to solve for general nonlinear dynamical systems  $p(\mathbf{x}' | \mathbf{x}, \mathbf{u}, \theta)$  and arbitrary forms of  $p(\theta)$ . Therefore, our approach is to solve the nested optimization via an iterative sequential programming approach which is regularized using an additional trust-region imposed on the outer policy optimization problem in Equation (2).

#### V. TRUST-REGION DISTRIBUTIONALLY ROBUST CONTROL

Introducing a trust-region over  $\pi_t$  has multiple advantages. On one hand, it regularizes the policy optimization step, which is crucial for convergence of the overall minimax problem. On the other hand, it offers a tractable maximum-entropy stochastic optimal control framework for dealing with nonlinear dynamics through successive linearization around a local trajectory distribution [20], [22].

The resulting overall approach alternates between updating the parameter and policy distribution. For every iteration  $k$ , we compute the updated worst-case distribution  $p^{k+1}$  given the ambiguity set  $\mathcal{B}_\delta$  around the nominal  $\hat{p}$ , and policy  $\pi_t^k$

$$p^{k+1} = \arg \max_{p \in \mathcal{B}_\delta(\hat{p})} J(\pi_t^k, p), \quad (4)$$

then we compute the updated robust policy  $\pi_t^{k+1}$  under  $p^{k+1}$  in a trust-region  $\mathcal{B}_\varepsilon$  around the old policy  $\pi_t^k$

$$\pi_t^{k+1} = \arg \min_{\pi_t \in \mathcal{B}_\varepsilon(\pi_t^k)} J(\pi_t, p^{k+1}). \quad (5)$$

**Algorithm 2: Worst-Case Parameter Optimization**

**input :**  $\hat{p}, \pi_t^k, \hat{\mu}_1, c_t, f, \delta$   
**initialize :**  $\beta$   
 $q_t \leftarrow \text{paramForPass}(\hat{p}, \pi_t^k, f, \hat{\mu}_1)$   
**while**  $F$  is not at minimum **do**  
  **repeat**  
     $p_t^{k+1}, V_t^\theta \leftarrow \text{paramBackPass}(q_t, \pi_t^k, c_t, f, \beta)$   
     $\mu_t \leftarrow \text{paramForPass}(p_t^{k+1}, \pi_t^k, f, \hat{\mu}_1)$   
     $q_t \leftarrow \lambda \mu_t + (1 - \lambda) q_t$   
  **until**  $\text{KL}(q_t || \mu_t) \approx 0$   
   $\frac{\partial F}{\partial \beta} \leftarrow \text{computeBetaGradient}(p_t^{k+1}, \hat{p}, \delta)$   
   $\beta \leftarrow \beta - \eta \frac{\partial F}{\partial \beta}$   
**output :**  $p_t^{k+1}, \mu_t$

These steps can also be seen as trust-region versions of the proximal updates performed by the mirror descent algorithm [23]. Algorithm 1 offers a schematic view of the optimization. The following sections provide further details.

**A. Worst-Case Parameter Distribution**

The parameter distribution optimization (4) for a single iteration  $k$  is given by

$$\begin{aligned} \underset{p_t}{\text{maximize}} \quad & \sum_{t=1}^{T-1} \iint c_t(\mathbf{x}, \mathbf{u}) \mu_t(\mathbf{x}) \pi_t^k(\mathbf{u}|\mathbf{x}) d\mathbf{x} d\mathbf{u} \quad (6a) \\ & + \int c_T(\mathbf{x}) \mu_T(\mathbf{x}) d\mathbf{x}, \end{aligned}$$

$$\begin{aligned} \text{subject to} \quad & \iiint \mu_t(\mathbf{x}) \pi_t^k(\mathbf{u}|\mathbf{x}) f(\mathbf{x}'|\mathbf{x}, \mathbf{u}, \boldsymbol{\theta}) \\ & \times p_t^{k+1}(\boldsymbol{\theta}) d\mathbf{u} d\mathbf{x} d\boldsymbol{\theta} = \mu_{t+1}(\mathbf{x}'), \end{aligned} \quad (6b)$$

$$\sum_{t=1}^{T-1} \text{KL}(p_t^{k+1}(\boldsymbol{\theta}) || \hat{p}(\boldsymbol{\theta})) \leq \delta, \quad (6c)$$

$$\int p_t^{k+1}(\boldsymbol{\theta}) d\boldsymbol{\theta} = 1, \quad \mu_1(\mathbf{x}) = \hat{\mu}_1(\mathbf{x}). \quad (6d)$$

Notice that we have moved to a time-variant worst-case parameter distribution  $p_t(\boldsymbol{\theta})$ . Although this formulation is more general, it is crucial to make this assumption in order to disentangle the adversary's influence over time and restrict it to future time steps. This modification makes sense when considering that the robust policy  $\pi_t(\mathbf{a}|\mathbf{s})$  is likewise time-variant and only influences the current and future time steps.

By solving the former primal problem using the method of Lagrangian multipliers [24], we arrive at the optimal worst-case parameter distribution  $p^{k+1}$

$$p_t^{k+1}(\boldsymbol{\theta}) \propto \hat{p}(\boldsymbol{\theta}) \exp \left[ -\frac{1}{\beta} W_t(\boldsymbol{\theta}) \right], \quad (7)$$

a softmax distribution with a temperature  $\beta \leq 0$  that corresponds to the trust-region constraint in Equation (6c) and a parameter value function  $W_t(\boldsymbol{\theta})$

$$W_t = \iiint V_{t+1}^\theta(\mathbf{x}') \mu_t(\mathbf{x}) \pi_t^k(\mathbf{u}|\mathbf{x}) f(\mathbf{x}'|\mathbf{x}, \mathbf{u}, \boldsymbol{\theta}) d\mathbf{u} d\mathbf{x} d\mathbf{x}',$$

**Algorithm 3: Dist. Robust Policy Optimization**

**input :**  $\pi_t^k, p_t^{k+1}, \hat{\mu}_1, c_t, f, \varepsilon$   
**initialize :**  $\alpha$   
**while**  $G$  is not at maximum **do**  
   $\pi_t^{k+1}, V_t^\pi \leftarrow \text{policyBackPass}(p_t^{k+1}, c_t, f, \alpha)$   
   $\mu_t \leftarrow \text{policyForPass}(p_t^{k+1}, \pi_t^{k+1}, f, \hat{\mu}_1)$   
   $\frac{\partial G}{\partial \alpha} \leftarrow \text{computeAlphaGradient}(\pi_t^{k+1}, \pi_t^k, \varepsilon, \mu_t)$   
   $\alpha \leftarrow \alpha + \rho \frac{\partial G}{\partial \alpha}$   
**output :**  $\pi_t^{k+1}, \mu_t$

where  $V_{t+1}^\theta(\mathbf{x}')$  is the Lagrangian function associated with Equation (6b) and acts as an adversarial state-value function under the last policy  $\pi_t^k(\mathbf{u}|\mathbf{x})$ .

By plugging the solution in Equation (7) back into the primal problem, we retrieve the dual  $F$  as a function of  $\mu$ ,  $V^\theta$  and  $\beta$

$$\begin{aligned} F = & \sum_{t=1}^{T-1} \iint c_t(\mathbf{x}, \mathbf{u}) \mu_t(\mathbf{x}) \pi_t^k(\mathbf{u}|\mathbf{x}) d\mathbf{u} d\mathbf{x} \\ & + \int c_T(\mathbf{x}) \mu_T(\mathbf{x}) d\mathbf{x} + \int V_1^\theta(\mathbf{x}) \hat{\mu}_1(\mathbf{x}) d\mathbf{x} \\ & - \sum_{t=1}^{T-1} \int V_t^\theta(\mathbf{x}') \mu_t(\mathbf{x}') d\mathbf{x}' - \int V_T^\theta(\mathbf{x}') \mu_T(\mathbf{x}') d\mathbf{x}' - \beta \delta \\ & - \beta \sum_{t=1}^{T-1} \log \int \hat{p}(\boldsymbol{\theta}) \exp \left[ -\frac{1}{\beta} W_{t+1}(\boldsymbol{\theta}) \right] d\boldsymbol{\theta}. \end{aligned}$$

We set the partial derivative of the dual w.r.t.  $\mu_t(\mathbf{x})$  to zero and get a backward recursion for computing  $V_t^\theta(\mathbf{x})$

$$\begin{aligned} V_t^\theta(\mathbf{x}) = & \iiint V_{t+1}^\theta(\mathbf{x}') \pi_t^k(\mathbf{u}|\mathbf{x}) f(\mathbf{x}'|\mathbf{x}, \mathbf{u}, \boldsymbol{\theta}) \\ & \times p_t^{k+1}(\boldsymbol{\theta}) d\boldsymbol{\theta} d\mathbf{u} d\mathbf{x}' + \int c_t(\mathbf{x}, \mathbf{u}) \pi_t^k(\mathbf{u}|\mathbf{x}) d\mathbf{u} \end{aligned}$$

where  $V_T(\mathbf{x}) = c_T(\mathbf{x})$ . Similarly, setting the partial derivative of the dual w.r.t.  $V^\theta$  to zero delivers a forward recursion for  $\mu_t(\mathbf{x})$

$$\mu_{t+1} = \iiint \mu_t(\mathbf{x}) \pi_t^k(\mathbf{u}|\mathbf{x}) f(\mathbf{x}'|\mathbf{x}, \mathbf{u}, \boldsymbol{\theta}) p_t^{k+1}(\boldsymbol{\theta}) d\mathbf{u} d\mathbf{x} d\boldsymbol{\theta},$$

where the initial state distribution  $\mu_1(\mathbf{x}) = \hat{\mu}_1(\mathbf{x})$  which is assumed given.

Finally, the optimal temperature  $\beta$  that satisfies the trust-region in Equation (6c) is optimized numerically via gradient descent on the dual where

$$\beta^{i+1} = \beta^i - \eta_i \sum_{t=1}^{T-1} \text{KL}(p_t^{k+1}(\boldsymbol{\theta}) || \hat{p}(\boldsymbol{\theta})) + \eta_i \delta,$$

and  $\eta_i$  is some step size. This process iterates over  $\mu$ ,  $V^\theta$  and  $\beta$  until convergence, see Algorithm 2. Given the circular dependency between  $V^\theta$ ,  $\mu$  and  $p$ , we update  $\mu$  through a barycentric interpolation scheme, analogous to [25].



## B. Worst-Case Robust Policy

Imposing a trust-region constraint on the robust stochastic optimal control formulation in (2) results in the following optimization problem

$$\underset{\pi_t}{\text{minimize}} \quad \sum_{t=1}^{T-1} \iint c_t(\mathbf{x}, \mathbf{u}) \mu_t(\mathbf{x}) \pi_t^{k+1}(\mathbf{u}|\mathbf{x}) d\mathbf{x} d\mathbf{u} \quad (8a)$$

$$+ \int c_T(\mathbf{x}) \mu_T(\mathbf{x}) d\mathbf{x},$$

$$\text{subject to} \quad \iint \mu_t(\mathbf{x}) \pi_t^{k+1}(\mathbf{u}|\mathbf{x}) f(\mathbf{x}'|\mathbf{x}, \mathbf{u}, \boldsymbol{\theta}) \times p_t^{k+1}(\boldsymbol{\theta}) d\mathbf{u} d\mathbf{x} d\boldsymbol{\theta} = \mu_{t+1}(\mathbf{x}'), \quad (8b)$$

$$\sum_{t=1}^{T-1} \int \mu_t(\mathbf{x}) \text{KL}(\pi_t^{k+1} || \pi_t^k) d\mathbf{x} \leq \varepsilon, \quad (8c)$$

$$\int \pi_t^{k+1}(\mathbf{u}|\mathbf{x}) d\mathbf{u} = 1, \quad \mu_1(\mathbf{x}) = \hat{\mu}_1(\mathbf{x}). \quad (8d)$$

By formulating the Lagrangian and solving for the robust policy  $\pi_t^{k+1}$ , we find

$$\pi_t^{k+1}(\mathbf{u}|\mathbf{x}) \propto \pi_t^k(\mathbf{u}|\mathbf{x}) \exp \left[ -\frac{1}{\alpha} Q_t(\mathbf{x}, \mathbf{u}) \right], \quad (9)$$

where  $Q_t(\mathbf{x}, \mathbf{u})$  is the state-action value function

$$Q_t = c_t(\mathbf{x}, \mathbf{u}) + \iint V_{t+1}^\pi(\mathbf{x}') f(\mathbf{x}'|\mathbf{x}, \mathbf{u}, \boldsymbol{\theta}) p_t^{k+1}(\boldsymbol{\theta}) d\boldsymbol{\theta} d\mathbf{x}'.$$

The temperature parameter  $\alpha \geq 0$  and function  $V_t^\pi(\mathbf{x})$  are the Lagrangian variables associated with Equation (8c) and Equation (8b).

Substituting Equation (9) back into the primal delivers the policy dual function  $G$

$$\begin{aligned} G = & \int c_T(\mathbf{x}) \mu_T(\mathbf{x}) d\mathbf{x} + \int V_1^\pi(\mathbf{x}) \hat{\mu}_1(\mathbf{x}) d\mathbf{x} \\ & - \sum_{t=1}^{T-1} \int V_t^\pi(\mathbf{x}') \mu_t(\mathbf{x}') d\mathbf{x}' - \int V_T^\pi(\mathbf{x}') \mu_T(\mathbf{x}') d\mathbf{x}' - \alpha \varepsilon \\ & - \alpha \sum_{t=1}^{T-1} \int \pi_t^k(\mathbf{u}|\mathbf{x}) \exp \left[ -\frac{1}{\alpha} Q_{t+1}^\pi(\mathbf{x}, \mathbf{u}) \right] d\mathbf{u} d\mathbf{x}. \end{aligned}$$

By setting the derivatives of  $G$  w.r.t.  $\mu_t(\mathbf{x})$  to zero, we arrive at an optimality condition in form of a backward recursion for calculating  $V_t^\pi(\mathbf{x})$

$$V_t^\pi(\mathbf{x}) = \alpha \log \int \pi_t^k(\mathbf{u}|\mathbf{x}) \exp \left[ -\frac{1}{\alpha} Q_t(\mathbf{x}, \mathbf{u}) \right] d\mathbf{u}, \quad (10)$$

where  $V_T^\pi = c_T(\mathbf{x})$ . On the other hand, the derivatives of  $G$  w.r.t.  $V^\pi(\mathbf{x})$  lead to a forward recursion for  $\mu_t(\mathbf{x})$  that fulfills the propagation constraint

$$\mu_{t+1} = \iint \mu_t(\mathbf{x}) \pi_t^{k+1}(\mathbf{u}|\mathbf{x}) f(\mathbf{x}'|\mathbf{x}, \mathbf{u}, \boldsymbol{\theta}) p_t^{k+1}(\boldsymbol{\theta}) d\mathbf{u} d\mathbf{x} d\boldsymbol{\theta}.$$

Similar to the optimization in Section V-A, the temperature  $\alpha$  is optimized via gradient ascent on the policy dual with

$$\alpha^{i+1} = \alpha^i + \rho_i \sum_{t=1}^{T-1} \int \mu_t(\mathbf{x}) \text{KL}(\pi_t^{k+1} || \pi_t^k) d\mathbf{x} - \rho_i \varepsilon,$$

where  $\rho_i$  is an adaptive step size. We refer to [26] for the convergence properties of trust-region optimization and specific rules for choosing and adapting the size  $\varepsilon$ . Algorithm 3 gives an outline of the overall optimization procedure.

## VI. PRACTICAL REALIZATION CONDITIONS

The recursive optimality conditions in Section V-A and Section V-B offer a general solution to the optimization problems without any guarantees for computational tractability. In this section, we discuss the assumptions necessary so that the proposed forward and backward passes are feasible.

### A. Linearized Quadratic Systems

Firstly, we assume a linear dynamics with a Gaussian additive noise

$$f(\mathbf{x}'|\mathbf{x}, \mathbf{u}, \boldsymbol{\theta}) = \mathcal{N}(\mathbf{x}'|\boldsymbol{\Theta}\boldsymbol{\tau}, \boldsymbol{\Sigma}_{\mathbf{x}'}),$$

where  $\boldsymbol{\Theta} = [\mathbf{A}, \mathbf{B}, \mathbf{c}]$  is the aggregate linear parameter matrix and  $\boldsymbol{\tau} = [\mathbf{x}, \mathbf{u}, \mathbf{1}]^\top$  is the combined state-action vector. Moreover, the cost functions  $c(\mathbf{x}, \mathbf{u})$  are presumed quadratic in state and action. Finally, the nominal parameter distribution is a Gaussian density  $\hat{p}(\boldsymbol{\theta}) = \mathcal{N}(\boldsymbol{\theta}|\boldsymbol{\mu}_\theta, \boldsymbol{\Sigma}_\theta)$ . Under these assumptions, the following holds

- 1) The state- and parameter-value functions  $V^\pi$  and  $V^\theta$  start at time  $T$  as quadratic functions and remain as such during the backward recursion due to the functional compatibility with the Gaussian probabilistic dynamics.
- 2) The resulting policy is a time-variant linear Gaussian  $\pi_t(\mathbf{u}|\mathbf{x}) = \mathcal{N}(\mathbf{u}|\mathbf{K}_t\mathbf{x} + \mathbf{k}_t, \boldsymbol{\Sigma}_{u,t})$ , where  $(\mathbf{K}_t, \mathbf{k}_t)$  are the linear feedback matrix and affine offset.
- 3) The optimal time-variant worst-case distribution  $p_t$  is a Gaussian density.
- 4) Propagation of the state through probabilistic dynamics results in a non-Gaussian distribution, due to the expectation over  $p_t(\boldsymbol{\theta})$ . We circumvent this issue by approximating the forwards recursion via spherical cubature.

This setting can be extended to support nonlinear dynamical systems and non-convex costs via local approximations. This approach mirrors the iterative linearization and quadratization scheme used in dynamic differential programming (DDP) [1] and iterative linear quadratic regulator (iLQR) [21], albeit with a more principled regularization achieved through the trust-region constraint on the policy [20]. Note that this extension requires a new reference nominal distribution  $\hat{p}^k(\boldsymbol{\theta})$  for every linearization iteration  $k$ , which we assume is given by an external statistical learning process.

### B. Cubature-Based State Propagation

We discuss the details of the approximate cubature forward recursion. The state propagation adheres to the probabilistic dynamics constraint

$$\mu(\mathbf{x}') = \iint \mu(\mathbf{x}) \pi(\mathbf{u}|\mathbf{x}) f(\mathbf{x}'|\mathbf{x}, \mathbf{u}, \boldsymbol{\theta}) p(\boldsymbol{\theta}) d\mathbf{u} d\mathbf{x} d\boldsymbol{\theta}, \quad (11)$$

in which we omit the superscripts and subscripts for brevity. Under the assumptions introduced in the previous section, the expected dynamics can be written as

$$\begin{aligned} p(\mathbf{x}'|\mathbf{x}, \mathbf{u}) &= \int f(\mathbf{x}'|\mathbf{x}, \mathbf{u}, \boldsymbol{\theta}) p(\boldsymbol{\theta}) d\boldsymbol{\theta} \\ &= \int N(\mathbf{x}'|\boldsymbol{\Theta}\boldsymbol{\tau}, \boldsymbol{\Sigma}_x) N(\boldsymbol{\theta}|\boldsymbol{\mu}_\theta, \boldsymbol{\Sigma}_\theta) d\boldsymbol{\theta} \\ &= N(\mathbf{x}'|\mathbf{M}_\theta\boldsymbol{\tau}, \boldsymbol{\Sigma}_x + (\boldsymbol{\tau}^\top \otimes \mathbf{I}_\theta)^\top \boldsymbol{\Sigma}_\theta (\boldsymbol{\tau} \otimes \mathbf{I}_\theta)), \end{aligned}$$

where  $\mathbf{M}_\theta$  is defined as  $\boldsymbol{\mu}_\theta = \text{vec}(\mathbf{M}_\theta)$  with  $\text{vec}$  denoting the vectorization operator, the operator  $\otimes$  stands for the Kronecker product and  $\mathbf{I}_\theta$  is the identity matrix with size equal to the dimension of  $\boldsymbol{\theta}$ . We write the covariance as  $\boldsymbol{\Sigma}(\boldsymbol{\tau}) = \boldsymbol{\Sigma}_x + (\boldsymbol{\tau}^\top \otimes \mathbf{I}_\theta)^\top \boldsymbol{\Sigma}_\theta (\boldsymbol{\tau} \otimes \mathbf{I}_\theta)$ , the second term of which depends on both state and action through  $\boldsymbol{\tau}$ . This leads to the integral in Equation (11) being non-Gaussian. We use the cubature transform as described in [27], which constitutes a variant of the unscented transform [28], to approximate the propagated state distribution. Therefore, we rewrite the dynamics equivalently as

$$\mathbf{x}' = \mathbf{M}_\theta\boldsymbol{\tau} + \sqrt{\boldsymbol{\Sigma}(\boldsymbol{\tau})}\boldsymbol{\xi}, \quad \boldsymbol{\xi} \sim N(\mathbf{0}, \mathbf{I}),$$

where the matrix square root indicates the lower triangular Cholesky factor. If we include the noise  $\boldsymbol{\xi}$  in the augmented state  $\hat{\boldsymbol{\tau}} := [\mathbf{x}, \mathbf{u}, \boldsymbol{\xi}]^\top$ , the cubature computation resembles propagating an augmented distribution  $p(\hat{\boldsymbol{\tau}})$  through a nonlinear deterministic dynamics function where

$$\begin{aligned} p(\hat{\boldsymbol{\tau}}) &= \mu(\mathbf{x}|\mathbf{m}, \boldsymbol{\Sigma}_x) \pi(\mathbf{u}|\mathbf{K}\mathbf{x} + \mathbf{k}, \boldsymbol{\Sigma}_u) p(\boldsymbol{\xi}|\mathbf{0}, \mathbf{I}_x) \\ &= N\left(\begin{bmatrix} \mathbf{x} \\ \mathbf{u} \\ \boldsymbol{\xi} \end{bmatrix} \middle| \begin{bmatrix} \mathbf{m} \\ \mathbf{K}\mathbf{m} + \mathbf{k} \\ \mathbf{0} \end{bmatrix}, \begin{bmatrix} \boldsymbol{\Sigma}_x & \boldsymbol{\Sigma}_x\mathbf{K}^\top & \mathbf{0} \\ \mathbf{K}\boldsymbol{\Sigma}_x & \boldsymbol{\Sigma}_u + \mathbf{K}\boldsymbol{\Sigma}_x\mathbf{K}^\top & \mathbf{0} \\ \mathbf{0} & \mathbf{0} & \mathbf{I}_x \end{bmatrix}\right). \end{aligned}$$

This reformulation allows us to apply standard cubature rules to obtain the new approximate state distribution  $\mu(\mathbf{x}')$ .

### C. Existence of The Worst-Case Distribution

Given the assumptions in Section VI, it is possible to compute the worst-case parameter distribution  $p_t^*(\boldsymbol{\theta}) = N(\boldsymbol{\theta}|\boldsymbol{\Omega}_t^{-1}\boldsymbol{\omega}_t, \boldsymbol{\Omega}_t^{-1})$  in closed-form

$$\begin{aligned} \boldsymbol{\omega}_t &= \hat{\boldsymbol{\Lambda}}_\theta \hat{\boldsymbol{\mu}}_\theta - \frac{1}{\beta} (\mathbf{s}_{xu,t}^\top \otimes \mathbf{I}_x)^\top v_{t+1}^\theta, \\ \boldsymbol{\Omega}_t &= \hat{\boldsymbol{\Lambda}}_\theta + (\boldsymbol{\Sigma}_{xu,t} \otimes \mathbf{V}_{t+1}^\theta) \\ &\quad + \frac{2}{\beta} (\mathbf{s}_{xu,t}^\top \otimes \mathbf{I}_x)^\top \mathbf{V}_{t+1}^\theta (\mathbf{s}_{xu,t}^\top \otimes \mathbf{I}_x), \end{aligned}$$

where  $\hat{\boldsymbol{\mu}}_\theta$  and  $\hat{\boldsymbol{\Lambda}}_\theta$  are the mean and precision of the nominal distribution  $\hat{p}(\boldsymbol{\theta})$ ,  $\mathbf{V}^\theta$  and  $v^\theta$  are the quadratic and linear terms of the adversarial state-value function  $V^\theta$  and  $\mathbf{s}_{xu}$  is the state-action distribution mean. Considering that  $\beta \leq 0$  and  $V^\theta \geq 0$ , depending on  $\hat{\boldsymbol{\Lambda}}_\theta$ , there exists a value of  $\beta$ , for which  $\boldsymbol{\Omega}$  becomes a negative-definite matrix and the distribution  $p_t^*(\boldsymbol{\theta})$  does not exist anymore in a Gaussian form. To overcome such issues, we propose a variant of our algorithm that mimics the trust-region sequential quadratic programming method [26, Chapter 4, 18]. Instead of the  $p$ -update in (4), we iteratively

update the worst-case distribution over smaller trust regions, i.e., we perform

$$p^{k+1} = \max_{p \in \mathcal{B}_{\delta_k}(\hat{p}) \cap \mathcal{B}_{\delta_k}(p^k)} J(\pi^k, p),$$

where  $\mathcal{B}_{\delta_k}$  denotes the KL-divergence trust region  $\mathcal{B}_{\delta_k}(p^k) = \{p \mid \sum_{t=1}^{T-1} \text{KL}(p||p_t^k(\boldsymbol{\theta})) \leq \delta_k\}$ . In practice, this iterative update is performed until the constraint in (4) becomes active.

## VII. EMPIRICAL EVALUATION

We empirically evaluate the proposed distributionally robust control on a set of linear and nonlinear dynamical systems with uncertain dynamics. Without loss of generality, we limit the scope and assume the existence of a probabilistic dynamics model that has been won from data at an earlier stage and which can be linearized along a trajectory to deliver the probabilistic time-variant dynamics, i.e. the nominal distribution. Moreover, we limit the evaluation to a classic finite-horizon trajectory optimization scenario and do not consider a receding horizon control scheme.

The evaluation focuses on highlighting the performance of the distributionally robust controller, iteratively optimized under its worst-case distribution, in comparison to an uncertainty-aware optimal controller, optimized under the nominal distributional dynamics using only the policy optimization stage of our approach. We perform this comparison by using the worst-case parameter optimization to compute an optimal disturbance on the uncertainty-aware controller and subsequently evaluate the performance of both controllers under this disturbance. This comparison allows the assessment of both controllers under previously unseen distributional disturbances, since the worst-case attack on the uncertainty-aware controller may vary from the worst-case attack on the iteratively optimized robust controller. As evaluation criteria, we consider (1) the overall expected cost on a set of intermediate distributions between the nominal and worst-case, which we find using barycentric interpolation, (2) the induced trajectory distributions and (3) the allocation strategy of the disturbance budget over the complete trajectory distribution. The source code of an efficient implementation can be found under <https://github.com/hanyas/trajopt>.

### A. Uncertain Linear Dynamical System.

We consider a simple actuated mass-spring-damper linear system with a mass  $m = 1$  kg, a spring constant  $k = 0.01$  N/m, and a damping factor  $d = 0.1$  Ns/m. The linear differential equation has the form

$$\begin{bmatrix} \dot{x}_t \\ \ddot{x}_t \end{bmatrix} = \begin{bmatrix} 0 & 1 \\ -0.01 & -0.1 \end{bmatrix} \begin{bmatrix} x_t \\ \dot{x}_t \end{bmatrix} + \begin{bmatrix} 0 \\ 1 \end{bmatrix} u_t,$$

which is integrated in time for a horizon  $T = 75$  with a step size  $\Delta t = 0.01$  s. Moreover, we assume an initial distribution  $\mu_1(\mathbf{x})$  centered at  $\mathbf{x}_0 = \mathbf{0}$  with a diagonal standard deviation of  $\sigma_{x_0} = 1 \times 10^{-1}$  and a discrete-time zero-mean process noise with a diagonal standard deviation  $\sigma_x = 1 \times 10^{-2}$ . The aim is to drive the system towards a goal state  $\mathbf{x}_g = [1, 0]^\top$ , under a quadratic state-action cost with the matrices  $\mathbf{C}_x =$

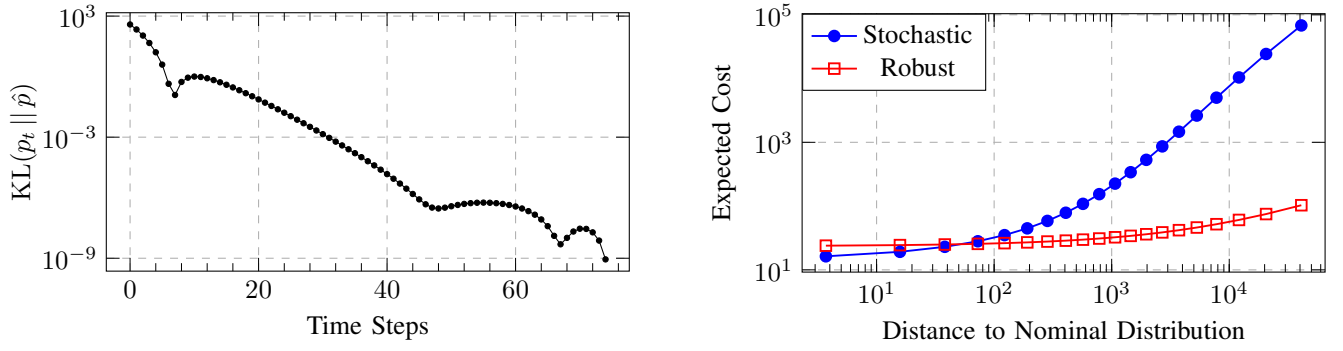


**Fig. 1:** Uncertain linear system experiment. Right, the worst-case KL budget allocation over the whole trajectory. Notice that most of the deviation happens in the first part of the trajectory. Left, the expected cost of the uncertainty-aware (blue) and robust (red) controllers evaluated on a range of distributions inter- and extrapolated between and beyond the nominal and worst-case distribution. The robust controller shows lower sensitivity to changes in the disturbance. Note the double logarithmic scale.

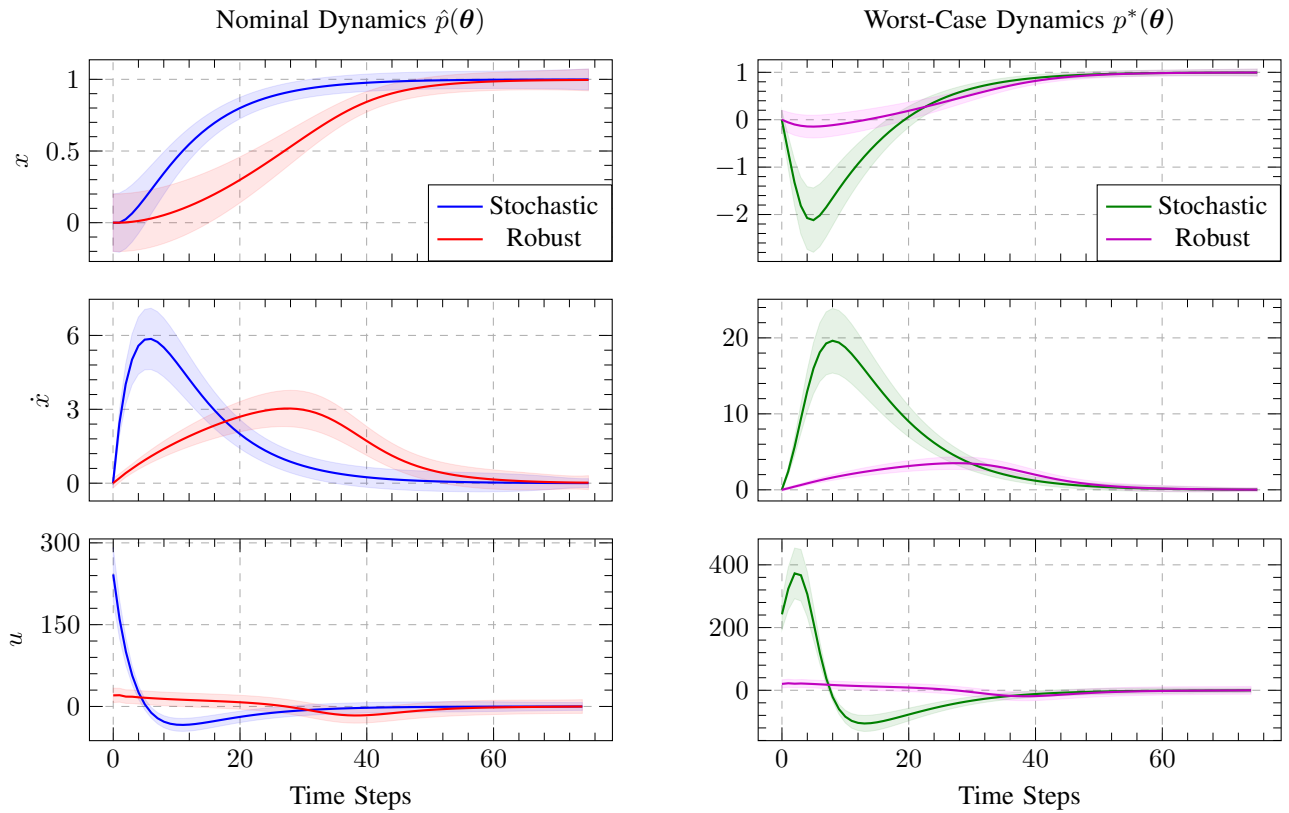


**Fig. 2:** Uncertain linear system experiment. Comparison between the uncertainty-aware and distributionally robust controllers. Left, the trajectory distributions induced by uncertainty-aware (blue) and robust (red) controllers evaluated under the nominal dynamics distribution. The uncertainty-aware controller is aggressive and reaches the target faster. Right, the trajectory distributions induced by uncertainty-aware (green) and robust (magenta) controllers evaluated under the worst-case disturbance. The uncertainty-aware controller overshoots dramatically beyond the target, while the robust controller shows is barely affected.

$\text{diag}([100, 0])$  and  $C_u = \text{diag}([0.001])$ . As stated previously, we assume the existence of a nominal distribution  $\hat{p}(\theta)$ , which in this case is centered at the true linear dynamics with a diagonal standard deviation of  $\sigma_\theta = 1 \times 10^{-4}$  to represent uncertainty over the parameters. We initialize a zero-mean controller with a diagonal standard deviation  $\sigma_\pi = 10$  and set the trust-region sizes  $\varepsilon = 0.25$  and  $\delta = 750$ .

The comparison between the controllers on the linear system

is depicted in Figure 2. The plots on the left show the trajectory distribution induced by the uncertainty-aware (blue) and robust (red) policies under the nominal parameter distribution  $\hat{p}(\theta)$ . The figures show an aggressive uncertainty-aware controller that takes full advantage of the nominal dynamics to reach the goal as fast as possible, while the robust controller shows sub-optimal behavior. However, when evaluated on the worst-case dynamics, on the right, the uncertainty-aware controller

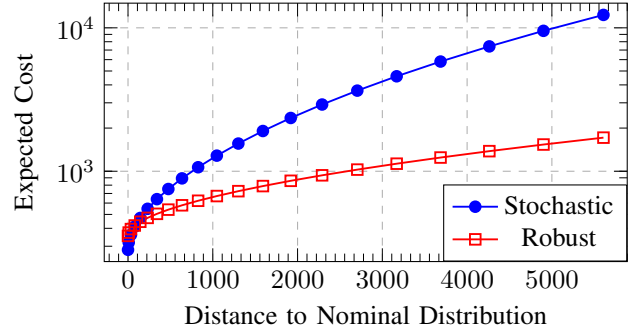
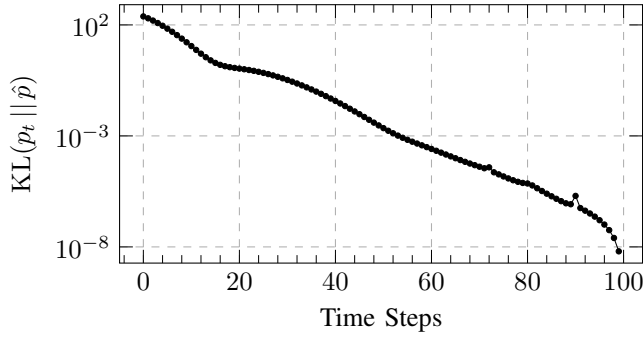


**Fig. 3:** Uncertain nonlinear robot experiment. Right, allocation of the worst-case KL budget over time steps. Most of the deviation is concentrated towards the early phase of the trajectory. Left, the expected cost of the uncertainty-aware (blue) and robust (red) controllers evaluated on a range of distributions inter- and extrapolated from the nominal and worst-case distribution: The robust controller shows much lower sensitivity to changes in the disturbance.

(green) overshoots beyond the target incurring a massive cost, while the robust policy (magenta) maintains a consistent behavior associated with much lower overall cost.

Furthermore, the right plot in Figure 1 illustrates the worst-case KL allocation over the trajectory. A large portion of the overall deviation takes place in the first 20 time steps, leading to the sub-optimal performance of the uncertainty-aware controller in the same time window. Finally, the left plot highlights the superior performance of the robust policy (red) on a continuum of distributions interpolated between the nominal and worst-case distributions and beyond using the method described in Appendix IX-A. The uncertainty-aware controller (blue) delivers better performance in a small region around the nominal distribution but very quickly worsens as the distance to that distribution increases.

### B. Uncertain Nonlinear Robot Car

This experiment validates our approach for general nonlinear dynamical systems via iterative linearization of the dynamics around a trust-region. We consider a nonholonomic robot moving in 2D-space. The state vector consists of the  $x, y$ -coordinates of the position, the speed  $v$  and the orientation  $\psi$ , while the acceleration  $a$  and the steering angle  $\phi$  are used for actuation. The global dynamics is nonlinear in state and action and given by

$$\begin{bmatrix} \dot{x}_t \\ \dot{y}_t \\ \dot{\psi}_t \\ \dot{v}_t \end{bmatrix} = \begin{bmatrix} v_t \sin \psi_t \\ v_t \cos \psi_t \\ v_t \tan(\phi_t)/d \\ a_t \end{bmatrix},$$

where constant  $d = 0.1$  m is the car length. This ODE is integrated for a horizon  $T = 100$  with a step size  $\Delta t = 0.025$  s. The initial state distribution is centered at  $[5, 5, 0, 0]^\top$  with a diagonal standard deviation  $\sigma_{x_0} = 1 \times 10^{-2}$  and the discrete-time process noise is zero-mean with a diagonal standard deviation  $\sigma_x = 1 \times 10^{-4}$ . The goal state is  $g = [0, 0, 0, 0]^\top$  and the quadratic cost function matrices are  $C_x = \text{diag}([10, 10, 1, 1])$  and  $C_u = \text{diag}([0.1, 0.1])$ . Analogous to the previous experiment, we assume the nominal parameter distribution to be centered at the linearized dynamics with a diagonal standard deviation  $\sigma_\theta = 1 \times 10^{-3}$ .

We initialize a zero-mean controller with a diagonal standard deviation  $\sigma_\pi = \sqrt{0.1}$  and set the trust-region radii to  $\varepsilon = 0.25$  and  $\delta = 500$ .

Figure 4 depicts the results in a similar fashion to what was presented in the last experiment. Here again, the uncertainty-aware controller (blue) acts aggressively under the nominal dynamics, while the robust controller (red) is slower and applies smaller controls. When evaluating the controllers under the uncertainty-aware controller's optimal adversary, the uncertainty-aware controller (green) overshoots and shows sub-optimal behavior while the trajectory distribution induced by the robust controller (magenta) is hardly affected. Lastly, the comparison of both controllers on a set of distributions interpolated between the nominal and the adversary highlights the overwhelming advantage of the robust controller, Figure 3.

## VIII. DISCUSSION

We have presented a technique to robustify data-driven stochastic optimal control approaches that rely on probabilistic models of the dynamics. Our approach consists of an iterative two-stage relative entropy trust-region optimization. The first stage optimizes the maximum entropy worst-case Gaussian distributional dynamics in a KL-ball around a nominal distribution, while the second stage optimizes the policy w.r.t. the worst-case dynamics. We show that for probabilistic time-variant dynamics models, both stages admit closed-form backward value recursions and approximate cubature forward passes. Empirical results on linear and nonlinear dynamical systems validate the benefits of robustifying stochastic control against worst-case statistical model disturbances.

Despite the encouraging initial results, our approach still has multiple limitations. The assumption of Gaussian densities for the nominal and worst-case distributions is rather limiting. Similarly, the restriction of the adversary to a time-variant form, although reasonable, does not reflect the nature of statistical errors that arise while approximating stationary representations of dynamics, as commonly used in the literature. In addition, long-horizon trajectory optimization is often prone to getting stuck in local minima. An investigation of a nonlinear model predictive control formulation can prove very beneficial, despite the additional computational load it may require. Finally, the KL divergence is not a proper distance



metric in the space of distributions. Analyzing the drawbacks of this design choice can inspire better alternatives, e.g., using kernel methods and optimal transport.

## IX. APPENDIX

### A. Barycentric Distribution Interpolation

Interpolating between two reference distributions  $p(x)$ ,  $q(x)$  in order to find an intermediate  $h(x)$  is done by minimizing the weighted Kullback-Leibler divergence objective

$$\arg \min_h \quad \lambda \text{KL}(h(x) || p(x)) + (1 - \lambda) \text{KL}(h(x) || q(x)),$$

subject to  $\int h(x) dx = 1,$

which results in an optimal distribution  $h^*(x)$

$$h^*(x) \propto q(x) \exp \left[ \lambda (\log p(x) - \log q(x)) \right],$$

which for Gaussians yields  $h^*(x) = \mathcal{N}(x | \mu^*, \Sigma^*)$

$$\Sigma^* = \left( \lambda \Sigma_p^{-1} + (1 - \lambda) \Sigma_q^{-1} \right)^{-1},$$

$$\mu^* = \Sigma^* \left( \lambda \Sigma_p^{-1} \mu_p + (1 - \lambda) \Sigma_q^{-1} \mu_q \right).$$

### B. Parameter Optimization

The Lagrangian function of the worst-case parameter optimization problem  $H(p, \mu, V^\theta, \beta, \gamma)$

$$\begin{aligned} H = & \sum_{t=1}^{T-1} \iint c_t(\mathbf{x}, \mathbf{u}) \mu_t(\mathbf{x}) \pi_t^k(\mathbf{u} | \mathbf{x}) d\mathbf{u} d\mathbf{x} \\ & + \int c_T(\mathbf{x}) \mu_T(\mathbf{x}) d\mathbf{x} + \int V_1^\theta(\mathbf{x}) \hat{\mu}_1(\mathbf{x}) d\mathbf{x} \\ & + \sum_{t=1}^{T-1} \int V_{t+1}^\theta(\mathbf{x}') \iiint \mu_t(\mathbf{x}) \pi_t^k(\mathbf{u} | \mathbf{x}) f(\mathbf{x}' | \mathbf{x}, \mathbf{u}, \boldsymbol{\theta}) \\ & \quad \times p_t^{k+1}(\boldsymbol{\theta}) d\mathbf{u} d\mathbf{x} d\boldsymbol{\theta} d\mathbf{x}' \\ & - \sum_{t=1}^{T-1} \int V_t^\theta(\mathbf{x}') \mu_t(\mathbf{x}') d\mathbf{x}' + \int V_T^\theta(\mathbf{x}') \mu_T(\mathbf{x}') d\mathbf{x}' \\ & + \beta \sum_{t=1}^{T-1} \int p_t^{k+1}(\boldsymbol{\theta}) \log \frac{p_t^{k+1}(\boldsymbol{\theta})}{\hat{p}(\boldsymbol{\theta})} d\boldsymbol{\theta} \\ & - \beta \delta + \sum_{t=1}^{T-1} \gamma_t \left( \int p_t^{k+1}(\boldsymbol{\theta}) d\boldsymbol{\theta} - 1 \right). \end{aligned}$$

Solving for optimal distribution  $p_t^{k+1}(\boldsymbol{\theta})$ , normalization variable  $\gamma_t$  leads to a simplified dual formulation

$$F = \int V_1^\theta(\mathbf{x}) \hat{\mu}_1(\mathbf{x}) d\mathbf{x} + \beta \sum_{t=1}^{T-1} \text{KL} \left( p_t^{k+1}(\boldsymbol{\theta}) || \hat{p}(\boldsymbol{\theta}) \right) - \beta \delta.$$

### C. Policy Optimization

The Lagrangian function of the robust policy optimization problem  $L(\pi, \mu, V^\pi, \alpha, \lambda)$

$$\begin{aligned} L = & \sum_{t=1}^{T-1} \iint c_t(\mathbf{x}, \mathbf{u}) \mu_t(\mathbf{x}) \pi_t^{k+1}(\mathbf{u} | \mathbf{x}) d\mathbf{u} d\mathbf{x} \\ & + \int c_T(\mathbf{x}) \mu_T(\mathbf{x}) d\mathbf{x} + \int V_1^\pi(\mathbf{x}) \hat{\mu}_1(\mathbf{x}) d\mathbf{x} \\ & + \sum_{t=1}^{T-1} \int V_{t+1}^\pi(\mathbf{x}') \iiint \mu_t(\mathbf{x}) \pi_t^{k+1}(\mathbf{u} | \mathbf{x}) f(\mathbf{x}' | \mathbf{x}, \mathbf{u}, \boldsymbol{\theta}) \\ & \quad \times p_t^{k+1}(\boldsymbol{\theta}) d\mathbf{u} d\mathbf{x} d\boldsymbol{\theta} d\mathbf{x}' \\ & - \sum_{t=1}^{T-1} \int V_t^\pi(\mathbf{x}') \mu_t(\mathbf{x}') d\mathbf{x}' - \int V_T^\pi(\mathbf{x}') \mu_T(\mathbf{x}') d\mathbf{x}' \\ & + \alpha \sum_{t=1}^{T-1} \iint \mu_t(\mathbf{x}) \pi_t^{k+1}(\mathbf{u} | \mathbf{x}) \log \frac{\pi_t^{k+1}(\mathbf{u} | \mathbf{x})}{\pi_t^k(\mathbf{u} | \mathbf{x})} d\mathbf{u} d\mathbf{x} \\ & - \alpha \varepsilon + \sum_{t=1}^{T-1} \int \lambda_t(\mathbf{x}) \left( \int \pi_t^{k+1}(\mathbf{u} | \mathbf{x}) d\mathbf{u} - 1 \right) d\mathbf{x}. \end{aligned}$$

Solving for optimal distribution  $\pi_t^{k+1}(\mathbf{u} | \mathbf{x})$  and normalization variable  $\lambda_t$  leads to the simplified dual formulation

$$G = \int V_1^\pi(\mathbf{x}) \hat{\mu}_1(\mathbf{x}) d\mathbf{x} - \alpha \varepsilon.$$

## REFERENCES

- [1] D. Mayne, "A second-order gradient method for determining optimal trajectories of nonlinear discrete-time systems," *International Journal of Control*, 1966.
- [2] S. Kamthe and M. Deisenroth, "Data-efficient reinforcement learning with probabilistic model predictive control," in *International Conference on Artificial Intelligence and Statistics*, 2018.
- [3] L. Hewing, A. Liniger, and M. N. Zeilinger, "Cautious nmpe with Gaussian process dynamics for autonomous miniature race cars," in *IEEE European Control Conference*, 2018.
- [4] H. Scarf, "A min-max solution of an inventory problem," *Studies in The Mathematical Theory of Inventory and Production*, 1958.
- [5] E. Delage and Y. Ye, "Distributionally robust optimization under moment uncertainty with application to data-driven problems," *Operations Research*, 2010.
- [6] B. P. Van Parys, D. Kuhn, P. J. Goulart, and M. Morari, "Distributionally robust control of constrained stochastic systems," *IEEE Transactions on Automatic Control*, 2015.
- [7] J. Coulson, J. Lygeros, and F. Dörfler, "Regularized and distributionally robust data-enabled predictive control," in *IEEE Conference on Decision and Control*, 2019.
- [8] I. Yang, "Wasserstein distributionally robust stochastic control: A data-driven approach," *IEEE Transactions on Automatic Control*, 2020.
- [9] J.-J. Zhu, W. Jitkrittum, M. Diehl, and B. Schölkopf, "Worst-case risk quantification under distributional ambiguity using kernel mean embedding in moment problem," in *IEEE Conference on Decision and Control*, 2020.
- [10] P. Coppens, M. Schuurmans, and P. Patrinos, "Data-driven distributionally robust lqr with multiplicative noise," in *Learning for Dynamics and Control*, 2020.
- [11] H. Rahimian and S. Mehrotra, "Distributionally robust optimization: A review," *arXiv preprint arXiv:1908.05659*, 2019.
- [12] Z. Hu and L. J. Hong, "Kullback-Leibler divergence constrained distributionally robust optimization," *Optimization Online*, 2013.
- [13] C. D. Charalambous and F. Rezaei, "Stochastic uncertain systems subject to relative entropy constraints: Induced norms and monotonicity properties of minimax games," *IEEE Transactions on Automatic Control*, 2007.
- [14] J. Peters, K. Mülling, and Y. Altun, "Relative entropy policy search," in *AAAI Conference on Artificial Intelligence*, 2010.

- [15] K. Kim and I. Yang, "Minimax control of ambiguous linear stochastic systems using the Wasserstein metric," in *IEEE Conference on Decision and Control*, 2020.
- [16] I. R. Petersen, M. R. James, and P. Dupuis, "Minimax optimal control of stochastic uncertain systems with relative entropy constraints," *IEEE Transactions on Automatic Control*, 2000.
- [17] H. Nishimura, N. Mehr, A. Gaidon, and M. Schwager, "RAT-iLQR: A risk auto-tuning controller to optimally account for stochastic model mismatch," *IEEE Robotics and Automation Letters*, 2021.
- [18] F. Farshidian and J. Buchli, "Risk sensitive, nonlinear optimal control: Iterative linear exponential-quadratic optimal control with Gaussian noise," *arXiv preprint arXiv:1512.07173*, 2015.
- [19] D. Nass, B. Belousov, and J. Peters, "Entropic risk measure in policy search," in *IEEE/RSJ International Conference on Intelligent Robots and Systems*, 2019.
- [20] S. Levine and V. Koltun, "Guided policy search," in *International Conference on Machine Learning*, 2013.
- [21] E. Todorov and W. Li, "A generalized iterative lqg method for locally-optimal feedback control of constrained nonlinear stochastic systems," in *IEEE American Control Conference*, 2005.
- [22] O. Arenz, H. Abdulsamad, and G. Neumann, "Optimal control and inverse optimal control by distribution matching," in *IEEE/RSJ International Conference on Intelligent Robots and Systems*, 2016.
- [23] A. Beck and M. Teboulle, "Mirror descent and nonlinear projected subgradient methods for convex optimization," *Operations Research Letters*, vol. 31, no. 3, pp. 167–175, 2003.
- [24] S. Boyd and L. Vandenberghe, *Convex Optimization*, 2004.
- [25] H. Abdulsamad, O. Arenz, J. Peters, and G. Neumann, "State-regularized policy search for linearized dynamical systems," in *International Conference on Automated Planning and Scheduling*, 2017.
- [26] J. Nocedal and S. Wright, *Numerical Optimization*, 2006.
- [27] A. Solin, "Cubature integration methods in nonlinear Kalman filtering and smoothing," 2010.
- [28] E. A. Wan, R. Van Der Merwe, and S. Haykin, "The unscented Kalman filter," *Kalman Filtering and Neural Networks*, 2001.

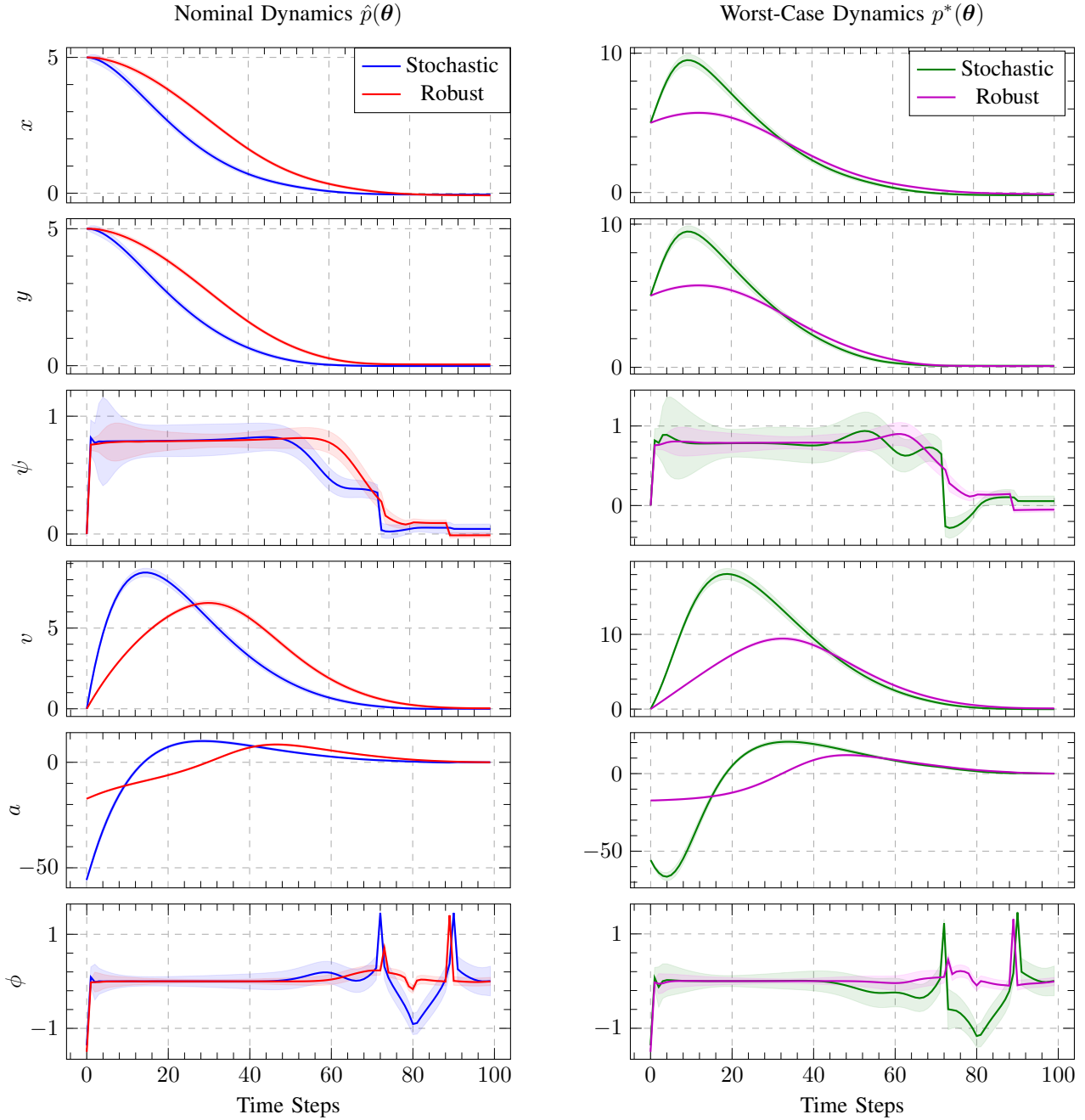


**Fig. 4:** Uncertain nonlinear robot experiment. Comparison of uncertainty-aware and distributionally robust controllers. Left, the trajectory induced by the uncertainty-aware (blue) and robust (red) controllers evaluated under the nominal dynamics distribution. The uncertainty-aware controller aggressively applies large controls to reach the target faster. Right, the trajectory distributions induced by uncertainty-aware (green) and robust (magenta) controllers evaluated under the worst-case disturbance. The uncertainty-aware controller shows clear sub-optimal behavior, while the robust controller is barely affected.